

## Shock-Front Irregularities in Polycrystalline Metals

M. A. MEYERS and M. S. CARVALHO

Instituto Militar de Engenharia, Centro de Pesquisa de Materiais, Pça. Gen. Tibúrcio, Urca, ZC-82, Rio de Janeiro, RJ (Brazil)

(Received February 9, 1976)

### SUMMARY

Shock waves in polycrystalline metals are characterized by irregularities in the front position as a result of the wave velocity dependence upon crystallographic orientation. A "wavy wave front" is consequently produced, and it is shown, by means of computer programming, that the irregularities increase as the wave penetrates into the metal.

### 1. INTRODUCTION

Shock waves are known to produce a variety of microstructural and substructural changes in metals, *e.g.* generation of point defects [1], dislocations [2] and twins [2], phase transformations [3] and precipitation [4]. The interaction of shock waves with existing defects is also of importance. Interactions with dislocations have been considered [5]; and grain-boundary ledges are known to be responsible for microcrack nucleation during the passage of shock waves [6].

Meyers [7] has recently shown, by means of mathematical calculations conducted for a simplified model, that the shock wave can assume a special configuration in polycrystalline metals. This special shape is characterized by irregularities in the front position, peak pressure and continuous emission of reflected waves and is the result of material anisotropy. The resultant "wavy wave" was suggested to have an effect on the residual substructure of the shock-loaded material. It is the purpose of this paper to show that the irregularities in the shock-front positions are accentuated as the wave progresses into the material.

### 2. CALCULATIONAL ASSUMPTIONS AND TECHNIQUES

The calculations were all conducted for a hypothetical situation: a nickel plate with grain size of 10  $\mu\text{m}$  being subjected to a plastic wave having an amplitude of 5 GPa (50 kbar).

There are two ways by which the velocities of the shock wave can be calculated; making the hydrodynamic assumption [8] or using an elastic-plastic treatment [9, 10]. For both methods the elastic constants are involved in the calculations, in spite of the fact that they have been determined for much lower stresses. The use is justified by the satisfactory correlation obtained between experimental and calculated data [9]. For the purpose of this paper it suffices to use the hydrodynamic assumption. The longitudinal components of the velocities of elastic waves along the three crystallographic orientations  $\langle 100 \rangle$ ,  $\langle 110 \rangle$ ,  $\langle 111 \rangle$  are presented by Ghatak and Kothari [11] in terms of the elastic stiffnesses  $c_{11}$ ,  $c_{12}$ ,  $c_{44}$  and the material density. The velocities of the longitudinal plastic waves are obtained from the assumption that the material cannot resist shear stresses, *i.e.*, that  $c_{44} = 0$ . The equations of Ghatak and Kothari [11] become (there are misprints in the original article):

$$U_{\langle 100 \rangle}^p = \sqrt{\frac{c_{11}}{\rho}}$$

$$U_{\langle 110 \rangle}^p = \sqrt{\frac{c_{11} + c_{12}}{2\rho}}$$

$$U_{\langle 111 \rangle}^p = \sqrt{\frac{c_{11} + 2c_{12}}{3\rho}}$$

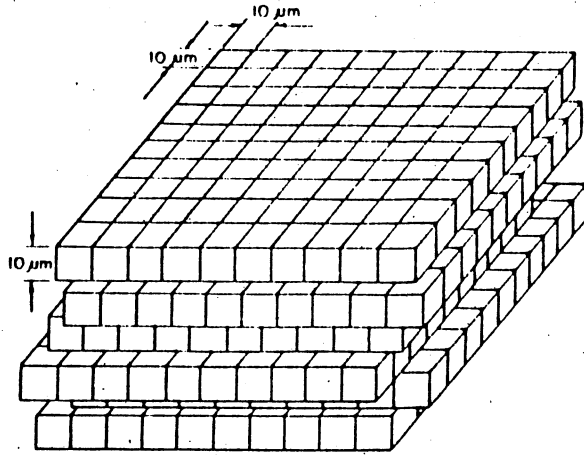


Fig. 1. Simplified configuration for the grains.

It is assumed that  $c_{11}$  and  $c_{12}$  retain their original values. This implies that the anisotropy ratio — defined as  $2c_{44}/(c_{11} - c_{12})$  — is altered. For nickel the values of the elastic stiffnesses are [11], at 300 K:

$$c_{11} = 2.508 \times 10^{11} \text{ Pa}$$

$$c_{12} = 1.500 \times 10^{11} \text{ Pa.}$$

The density of nickel at 5 PGa is given by its Hugoniot curve and is equal to  $9.07 \times 10^3 \text{ kg/m}^3$ . The transient temperature rise associated with the passage of the shock wave is neglected. Hence, the velocities of the shock wave for the hypothetical situation referred to previously are:

$$U_{<100>}^p = U_1 = 5.26 \times 10^3 \text{ m/sec}$$

$$U_{<110>}^p = U_2 = 4.70 \times 10^3 \text{ m/sec}$$

$$U_{<111>}^p = U_3 = 4.50 \times 10^3 \text{ m/sec.}$$

The velocity anisotropies calculated by the above procedure are consistent with the ones obtained by the elastic-plastic treatment [9]. The orientations  $\langle 100 \rangle$ ,  $\langle 110 \rangle$  and  $\langle 111 \rangle$  were coded 1, 2 and 3, respectively.

The shock-wave profile can be estimated at any position inside the nickel sheet, in various degrees of rigorourness. An approximate profile that does not require extensive mathematical manipulation can be produced by making some simplifying assumptions and specifying some parameters:

(a) All grains are cubes with  $10 \mu\text{m}$  sides, arranged in horizontal layers, as shown in Fig. 1. There is no exact superposition of the cubes. The shock wave is horizontal and traverses the material from top to bottom.

(b) It is assumed that there are only three vertical orientations for the grains:  $\langle 100 \rangle$ ,  $\langle 110 \rangle$  and  $\langle 111 \rangle$ . These are the sole orientations along which purely longitudinal waves exist [11, 12]. Assuming that the least texturing takes place, they will be present in proportion to their multiplicity factors; these are 6, 12 and 8 respectively. Consequently, the probabilities for the orientation of each grain are:

$$P_{\langle 100 \rangle} = p_1 = 0.461$$

$$P_{\langle 110 \rangle} = p_2 = 0.231$$

$$P_{\langle 111 \rangle} = p_3 = 0.308.$$

The transit times of the wave for the grains of three orientations are  $t_1$ ,  $t_2$  and  $t_3$  and are given below:

$$t_{\langle 100 \rangle} = t_1 = \frac{10^{-5}}{U_1} = 1.90 \times 10^{-9} \text{ sec}$$

$$t_{\langle 110 \rangle} = t_2 = \frac{10^{-5}}{U_2} = 2.13 \times 10^{-9} \text{ sec}$$

$$t_{\langle 111 \rangle} = t_3 = \frac{10^{-5}}{U_3} = 2.22 \times 10^{-9} \text{ sec.}$$

On the basis of these assumptions, the problem of determining a shock-front profile is more easily solved in two stages. Firstly one calculates the probability distribution function of the transit times for a certain penetration corresponding to  $n$  grains. The problem can be statistically stated as: what is the probability distribution function of  $n$  indistinguishable events 1, 2 and 3, with probabilities  $p_1$ ,  $p_2$  and  $p_3$  and values  $t_1$ ,  $t_2$  and  $t_3$ ? One has to determine the number of possible configurations  $C$  of  $n_1$  events of type 1,  $n_2$  events of type 2 and  $n_3$  events of type 3 ( $n_1 + n_2 + n_3 = n$ ):

$$C = \frac{n!}{n_1! n_2! n_3!}.$$

The probability  $P$  of each outcome is:

$$P = p_1^{n_1} \times p_2^{n_2} \times p_3^{n_3}.$$

The total probability of each outcome is the product of  $C$  versus  $P$ . The transit time of each outcome is given by the sum of the transit times  $t_1$  of the  $n_1$  grains of type 1,  $t_2$  of the  $n_2$  grains of type 2 and  $t_3$  of the  $n_3$

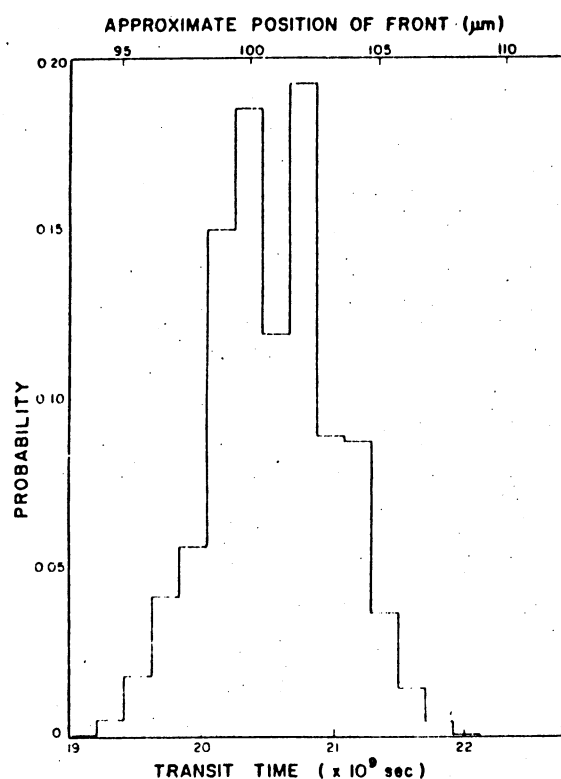


Fig. 2. Distributions of transit times and shock-front positions for a mean penetration of 10 grains.

grains of type 3. Such a plot is shown in Fig. 2, for  $n = 10$ . The transit times are grouped in intervals of  $0.2 \times 10^{-9}$  sec.

Secondly, what is done is to determine the position distribution function. An approximate position distribution function, at the instant when the mean of the wave has traversed  $n$  grains, can be computed by assuming a weighed average of velocities:

$$U_{av} = p_1 U_1 + p_2 U_2 + p_3 U_3 = 4.90 \times 10^3 \text{ m/sec.}$$

Multiplying this velocity by the limits of the time intervals, one obtains the positions. The upper abscissa in Fig. 2 provides the distribution of these positions. It is to be noted that the above calculation is merely an approximation. However, sensible deviations only occur at the tails of the distribution of Fig. 2; they are therefore of no great concern.

The position distribution functions shown in Fig. 2 and subsequent ones were obtained from data processed in an IBM 1130 computer. Since the data were grouped in the same intervals for all the plots ( $0.2 \times 10^{-9}$  sec), they can be directly compared.

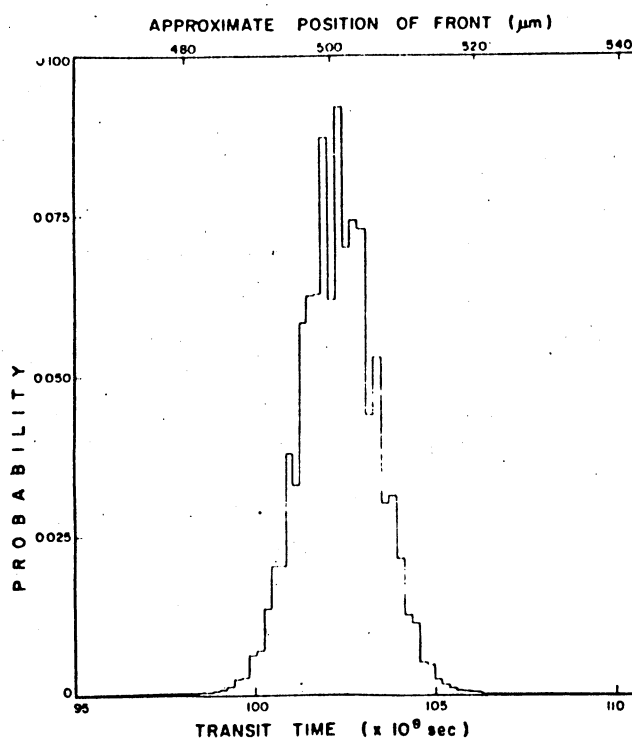


Fig. 3. Distribution of transit times and shock-front positions for a mean penetration of 50 grains.

### 3. RESULTS AND DISCUSSION

The variation in the distribution of transit times and shock front position, as the wave traverses the material, is shown in Figs. 2 - 5. Two abscissae are shown in each Figure; the lower shows the transit times while the upper one presents the positions. Figures 2, 3, 4 and 5 are the distributions for  $n = 10, 50, 100$  and  $150$  respectively. The calculations were not continued beyond 150 grains because of the large processing times involved. For 150 grains the processing time was approximately four hours in the IBM 1130 computer. As the wave advances the distribution progressively broadens out. This broadening can be seen in Fig. 6, where the standard deviation of the position distribution is plotted against the penetration distance inside the material. So, when the wave is  $0.15$  mm inside the material, the standard deviation is already around  $8 \mu\text{m}$ , meaning that 68% of the wave is within  $16 \mu\text{m}$  band. These irregularities are larger than the grain size; consequently the grains are subjected to a stress state that is obviously very different from the one that would be imposed by a perfectly planar wave. It has

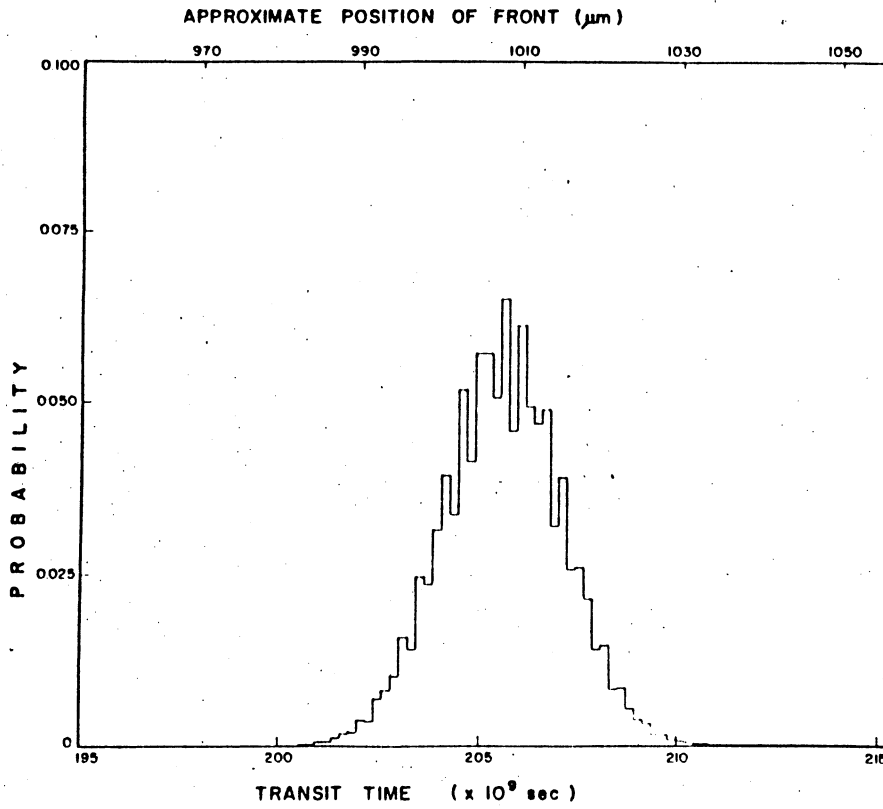


Fig. 4. Distribution of transit times and shock-front positions for a mean penetration of 100 grains.

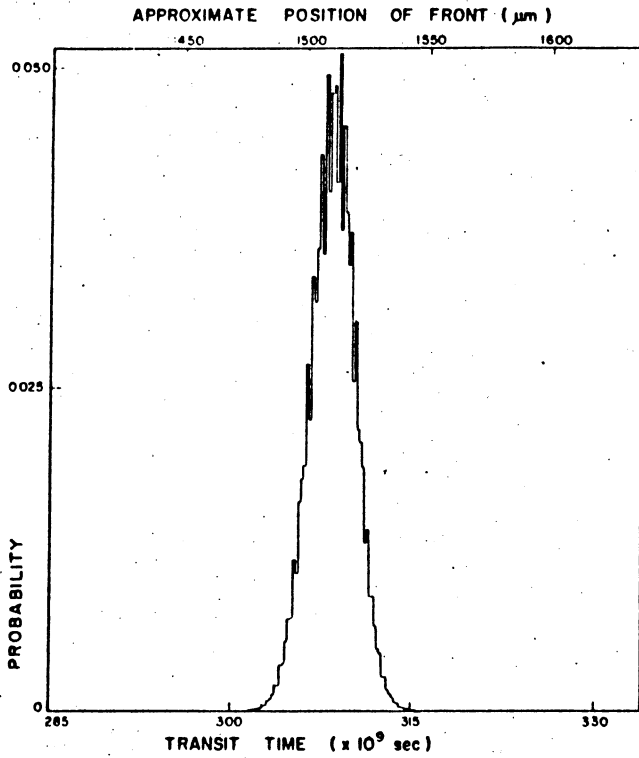


Fig. 5. Distribution of transit times and shock-front positions for a mean penetration of 150 grains.

Fig. 5. Distribution of transit times and shock-front positions for a mean penetration of 150 grains.

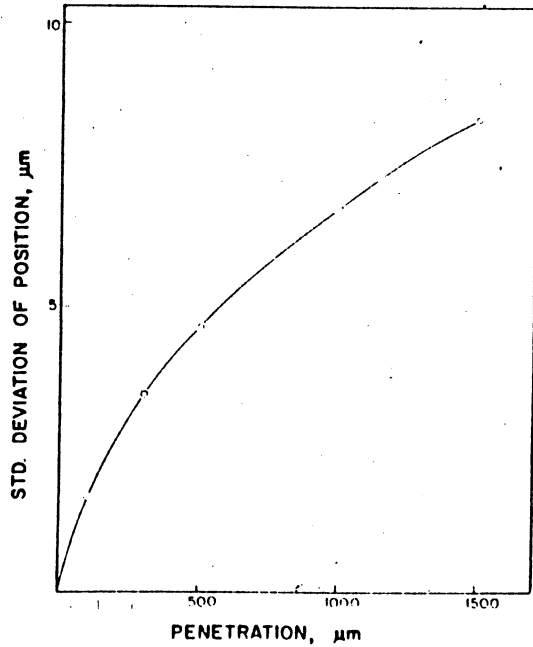


Fig. 6. Variation of the standard deviation in the shock-front position with the penetration distance of the wave into the material.

been shown [13] that irregularities introduced in the shock wave (by machining a pattern in the cover plate) can affect the residual

hardness of type 304 stainless steel. The model for the grains shown in Fig. 1 does not assume the vertical superposition of the cubic grains; consequently the wave splits itself after traversing each grain layer. Hence the irregularities in the shock-front positions become increasingly refined.

#### 4. CONCLUSION

It can be concluded from the simplified model presented herein that the irregularities in the shock-front position increase in amplitude as the wave penetrates into the material. These irregularities change the stress state at the shock front and should therefore affect the plastic strains and residual structure.

#### ACKNOWLEDGEMENTS

This work is supported by the Brazilian Army, FINEP, MEC and BNDE through IME Materials Research Center.

#### REFERENCES

- 1 H. Kressel and N. Brown, *J. Appl. Phys.*, 38 (1967) 1618.
- 2 D. C. Brillhart, R. J. De Angelis, A. G. Proban, J. B. Cohen and P. Gordon, *Trans. AIME*, 239 (1967) 836.
- 3 C. S. Smith, *Trans. AIME*, 212 (1958) 574.
- 4 C. Stein, *Scripta Met.*, 9 (1975) 67.
- 5 C. H. Ma, *Acta Met.*, 22 (1974) 675.
- 6 J. M. Galbraith and L. E. Murr, *J. Mater. Sci.*, 10 (1975) 2025.
- 7 M. A. Meyers, *Proc. 5th Intern. Conf. on High Energy Rate Fabrication*, Denver Res. Inst., 1975.
- 8 G. E. Dieter, *Strengthening Mechanisms in Solids*, Am. Soc. Metals, 1961, Chap. 10, p. 279.
- 9 J. N. Johnson, *J. Phys. Chem. Solids*, 35 (1974) 609.
- 10 E. H. Lee, in J. J. Burke and V. Weiss (eds.), *Shock Waves and the Mechanical Properties of Solids*, Syracuse University Press, 1971, p. 3.
- 11 A. K. Ghatak and L. S. Kothari, *An Introduction to Lattice Dynamics*, Addison-Wesley, 1972, p. 67.
- 12 W. Herrmann, D. L. Hicks and E. G. Young, source cited in Ref. 10, p. 23.
- 13 M. A. Meyers, *Scripta Met.*, 9 (1975) 667.